MONTE CARLO STUDY OF A MOSFET DETECTOR RESPONSE APPLIED TO X-RAY MICROBEAM RADIATION THERAPY

M. DE FELICI [A], R. FELICI[A], M. SANCHEZ DEL RIO [B],
A. DILMANIAN[C] AND C. FERRERO [B]

[a] *INFM-OGG c/o ESRF, BP220 F-38043-Grenoble Cedex*
[b] *ESRF, BP220 F-38043-Grenoble Cedex*
[c] *Medical Department, Brookhaven National Laboratory, Upton, NY 11973, USA*

EGS4 Monte Carlo calculations of the dose deposited by array of microbeams, used for the Microbeam Radiation Therapy technique, are presented. The sensitivity of the results to the experimental parameters (incident beam energy, beam array dimensions and spacing) has been assessed. The effects of the photon beam polarization and energy cut-off have also been investigated. The response of a Silicon MOSFET detector of micrometric dimensions, placed inside a phantom made of two homogeneous media (water and PMMA), has been simulated.

1. Introduction

Microbeam Radiation Therapy (MRT) is a pre-clinical technique, potentially useful for treating brain tumours of infancy, when other kinds of radiotherapy appear not to be safe. MRT is based on the use of arrays of parallel, microscopically thin planes of x-ray beams, resulting on a tissue-sparing effect /1,2/. Normal rat tissues display an unusual high resistance to necrosis when irradiated with such beams. This sparing effect might be ascribed to rapid repair of microscopic lesions by non-irradiated adjacent cells.

Multiple planar microbeams of uniform thickness (25-50 μm), spaced at intervals of 100 up to 200 μm, have been used for treating brain tumours in pre-clinical experiments. Preliminary results of microbeams shots extended considerably the average survival time of young adult rats bearing advanced intracerebral gliosarcomas, ablating the tumour in about half of them /1/. Histological examinations showed that sane tissue damage was minor or non-existent, suggesting the possibility of different dose effects between normal and tumour tissues.

At present MRT research programs require x-ray source characteristics, like photon flux and spectrum, which can only be supplied by wiggler insertion

devices at third generation synchrotron sources. Such kind of experiments are carried out either at the National Synchrotron Light Source (NSLS), Brookhaven National Laboratory (BNL), where the method was conceived in the early 1990s, and at the European Synchrotron Radiation Facility (ESRF).

Radiation damage of the tissues and sparing effects are related with the absolute doses in the peaks (along the track of the microbeam) and in valleys (between two adjacent peaks) regions, and with their ratio (peak-to-valley dose ratios, PVDR). Dose evaluation is a crucial aspect in radiation therapy. It involves either the direct measurement of the delivered dose and their validation by Monte Carlo simulations. In the case of MRT the measurement and the simulation of dose distributions from microbeam arrays have been a challenging topic since the advent of its concept. Simulation works were done by Slatkin et al. /3/ and Stepanek et al. /4/ while comparisons between MOSFET measurements and simulations in homogeneous can be found in Orion et al. /5/, and Bräuer-Krisch et al. /6/. The high requirements for accurate description of the synchrotron radiation beam characteristics (energy spectrum, polarization, source sizes and divergences, etc.), the complexity of the physical processes involved (electron and photon transport and interactions) and the geometry of the human head phantom, make these calculations extremely complex.

In this work we have used the EGS4 Monte Carlo code /7/ to compute the delivered dose for different microbeam geometries, with an emphasis on the PVDRs. The dependence of the distributions on parameters such as beam energy spectrum, array size, beam spacing, phantom size and composition, and the depth of the target volume in the phantom have been investigated. The response of the MOSFET silicon micro-detector used for the determination of the dose profile both from a single microbeam and an array of microbeams has been simulated.

2. Method and results

We have developed an EGS4 user code to perform simulations of microbeam dose distribution in simulated phantoms of different geometrical geometries and compositions. Like in other works dealing with the same subject /3,4/, we used a 16cm diameter, 16cm long, cylindrical phantom, to better compare our results with those published previously. The x-ray beam travelling along the z-axis impinges on the centre of one of the cylinder base.

Deposition of the x-ray microbeam dose in the tissue is mediated by photoelectrons, Compton electrons, and Auger electrons, which are produced, in

turn, by the primary photons as well as incoherently and coherently scattered photons and fluorescence x-rays.

Energy transport depends on the interaction potentials of x-ray and electrons with matter. Monte Carlo programs simulate the energy lost by these particles until their energy is lower than a predefined value. For energies lower than this cut-off energy the particle is considered fully stopped (absorbed) and all the remaining energy is deposited locally. From the point of view of energy transport, a photon can become at any moment an electron (photoemission) and vice versa an electron can become a photon (bremstrahlung). Therefore, the cut-off energies for the two particles should be set to equal values. To determine the best threshold values we studied their influence on the dose profile. For this purpose we used a 1 μm collimated, 50 keV monochromatic, unpolarised beam, and we calculated the dose deposited in a water phantom. Our calculation have shown that in order to have a spatial resolution of 1 μm the cut-off energies for electron ant photon trasport should be 500 eV or less.

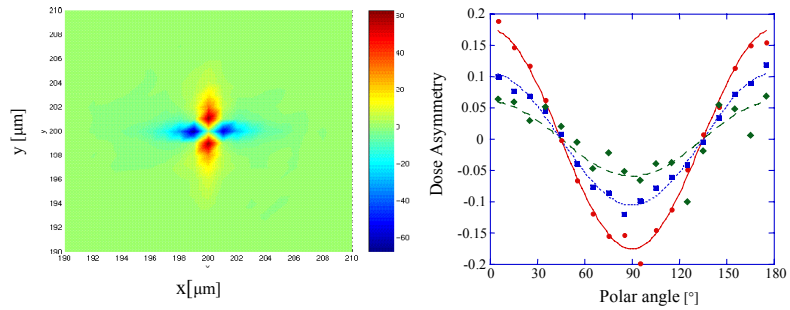

Fig.1 Left) Polarization effect on the dose deposited around a 50 keV pencil beam. The picture displays the percent difference between the doses calculated with the incident polarization along the "y" and "x" axis. Right) asymmetry ratio of the dose deposited by a 200 keV pencil beam integrated for different distances: circles range 0-50 μm, squares range 50-100 μm and diamonds range 100-150 μm. The lines are sinusoidal fit to the data.

Most of the x-ray interactions depend on the polarization of the incident radiation. Differently from standard medical x-ray or γ sources, synchrotron radiation is strongly polarised. In this work we have deeply studied the effect induced by the beam polarization in the Compton scattering, which is the photon dominant interaction in the energy range of interest for MRT. The Compton electrons play the major role in transporting the energy away from the directly illuminated region up to distances of about 100 microns. In order to illustrate the effect, we have computed the difference between two dose distributions produced by a linearly polarized monochromatic pencil beam, for two

perpendicular directions of the photon electric field (Fig.1). The doses have been calculated using the phantom previously described at depth between 7 and 8 cm from the surface. The results show that the dose difference is significant, reaching difference values of about 60%, near to the incident beam zone where the Compton electron contribution is predominant. On the right side we show the asymmetry ratio, calculated as the ratio of the dose difference with the dose sum, integrated over different distances for an incident pencil beam of 200 keV. In this case the created Compton electrons have higher energies and the asymmetry is still evident up to distances larger than 150 μm.

The polarization dependency can often be neglected in PVDR calculations at the centre of large beam arrays, made of hundreds of beams, with a spacing of about one hundred micrometers. In fact the centre receive doses coming from all the directions, averaging this effect. On the contrary, significant differences have been calculated at the side of the illuminated region, where dose asymmetries as large as 15% have been computed.

Monochromatic and pencil beams are never used for MRT purposes because they deposit too small doses to be effective. Arrays of planar beams have so far been considered. A routine able to simulate a single planar beam has been implemented in the code. We have checked the related results with those obtained with a pencil beam convoluted with a box distribution of the desired beam width

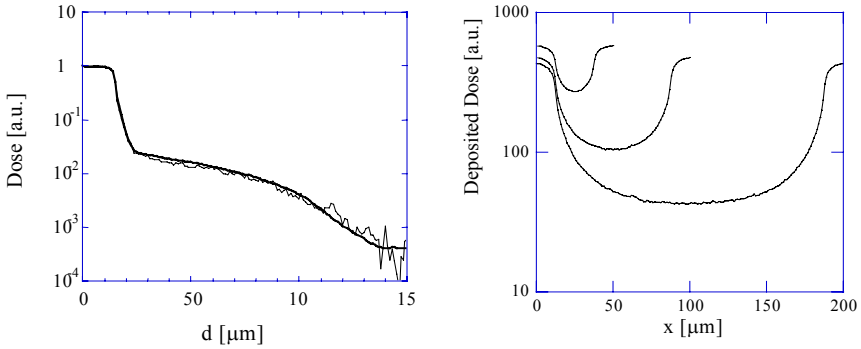

Fig.2 Left) Comparison between the planar beam (30 μm *300 μm) dose profile, calculated at a depth between 7 and 8 cm, as a function of the distance from the beam and that obtained by convolving the pencil beam on an equivalent rectangular region for a monochromatic incident beam of 50 keV. Right) Dose profile at the center of a 3x3 cm^2 microbeam array 25 μm thick for different beam spacings.

In order to perform realistic calculation of dose deposition which could be compared with the results of dosimetry experiments based on the use of a Silicon MOSFET detector, it is necessary to perform two more steps: a) fully

simulate the x-ray source, b) score the dose deposited in the geometric zone defined by the micro detector.

The x-ray beams are normally obtained from white spectra emitted by a bending magnet or an insertion device, usually a wiggler. The x-ray beam is then filtered to remove photons of low energies that are less effective for MRT purposes and increment the deposited dose in regions near the surface. For our calculations, we have used a spectral distribution calculated with the source parameters of the ID17 medical beam-line at the ESRF. It presents an effective energy flux ranging from about 50 keV (after filtering with 16mm of Al) up to energies higher than 300 keV.

The role of the detector geometry is crucial. In most of the published works dealing with MRT, the dose has been evaluated in a scoring volumes of the phantom made of a single homogenous material, either water or PMMA. In order to compare dosimetry calculations with measurements, we need to simulate the sensitive element used for scoring the doses. To evaluate the detector response in MRT, we simulated the dose deposited in a MOSFET silicon detector, placed at different depths inside the phantom and in different positions with respect to the microbeam array. As detector phantom we considered the silicon sensitive element, developed by Rosenfeld and already used in microbeams experiments /8/. The phantom is the homogenous cylinder made of water or PMMA . The detector is approximated by a silicon parallelepiped which can be freely positioned inside the cylinder.

We first calculated the dose deposited in the detector volume filled with the same material as the phantom and we compared these values to those ones previously reported. In the case of uniform phantom, the errors in the dose evaluation have been determined selecting regions at the “top” and at the “valley” of the dose profile, and then calculating the average and variance of the doses scored in these regions. Modelling a detector, which has a very small scoring volume, the average cannot be carried out with the same procedure, because the number of events in the sensitive elements is very small, and dividing it, in even smaller regions to perform the statistical analysis, is not possible. Here, we used a procedure based on the proportionality existing between the dose deposited in the detector and the number of incident photon histories. By plotting the dose deposited in the detector volume versus the number of tracked histories and using a least square fitting procedure, as we show in fig 4, the dose values with the associated errors can be determined. The scored doses well agree with the values calculated using the homogeneous phantom, giving us confidence on the possibility of using EGS4 even in the case of regions with micrometric dimensions.

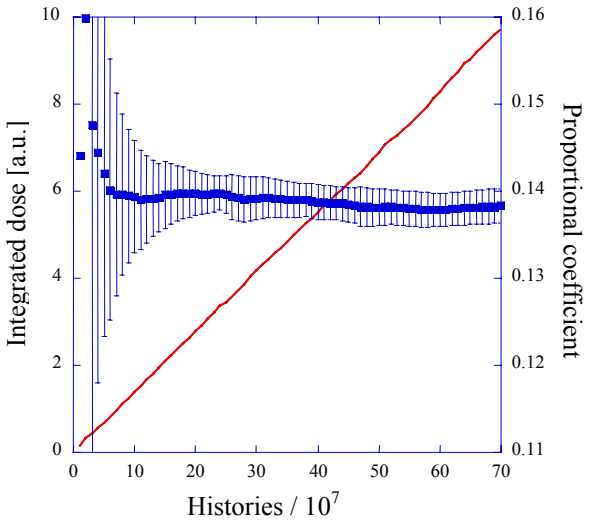

Fig.3) Dose scored in a Silicon detector placed in edge mode at a depth of 2 cm inside a cylinder PMMA phantom. The line is the accumulated dose as a function of the histories (left scale of the graph) while the points with the associated errors are the proportionality constant obtained by least square methods (right scale of the graph).

In Fig.4a we show the dose deposited in the Si detector using a single cylindrical 25μm diameter beam (points), and the dose profile calculated using an homogeneous phantom. Calculations have been carried for water and PMMA. The data have been normalized to one at the centre of the incident microbeam. A strong difference is present between the results calculated with water and PMMA. At a distance of 50 μm from the beam centre, the dose calculated in water is about twice as much as that in PMMA. Moreover the dose deposited in the Si detector, is always lower with respect to the one calculated for the homogenous water or PMMA media (without detector). The dose calculated with the Si detector simulation, at 50 μm distance, is about 2/3 of the correspondent dose calculated in the homogeneous medium. This effect can be induced by the larger ratio between the Si and the water or PMMA absorption photoelectric cross sections, when compared to the electron cross sections. As a consequence, a Si detector is more sensitive to the dose carried by photons with respect to the dose transported by electrons when compared to water and PMMA.

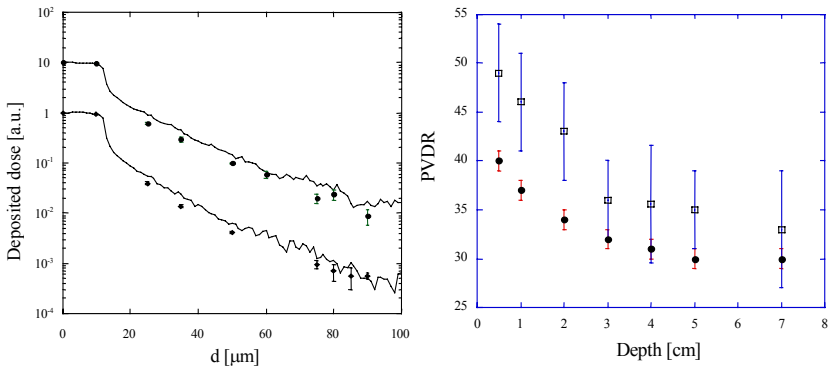

Fig.4 left) Dose deposited by a 25 μm diameter pencil at a depth of 7 cm in a phantom made of water (upper curve) or PMMA medium (lower curve). The points are the calculated doses deposited in a Si detector placed inside the phantom in "edge mode" geometry at 7 cm depth and at different distances from the incident beam's direction. The data have been normalized to one at the centre of the beam and the water data were shifted up by one decade for clarity resons. The error in the calculation, when not clearly shown, is less than the point dimension. Right) Peak-to-valley ratios calculated as a function of the depth in the phantom for a 1x1 cm^2 array of 25 μm planar microbeams with a spacing of 200 μm, for of a uniform water phantom (full circles), and for a Si detector placed within a PMMA medium (open squares).

Since the valley dose is a non-trivial superposition of the doses deposited either by electrons (vicinal microbeams) or by photons (far microbeams), the PVDR recorded by a Si detector strongly depends on the geometrical configuration of the planar microbeams, namely their vertical dimension, spacing, thickness and total number of beams.

As an example, we show in Fig.4b the PVDR, as a function of the depth, calculated in the case of a homogeneous water phantom and of a Si detector. The PVDR have been calculated at the centre of an array of 25μm planar microbeams, covering a region of 1x1 cm^2 and with a periodicity of 200 μm. The Si detector was placed inside a uniform PMMA phantom. Its dimensions were: 200 μm height, 200 μm depth and 2 μm thickness. It can be seen that the difference between the two sets of values amounts to more than 20% at depths less than 2 cm. The errors for the Si detector calculations are quite large because of the small amount of scored energy into the small detector volume. The error is dominated by the uncertainties in the valley dose. The calculations have been carried out using a cluster of 1GHz Pentium, 512 Mbyte RAM PC's. The calculation time for each point was of the order of 70 days.

3. Conclusions and perspectives.

We have verified that the polarization of the incident x-ray microbeams can induce important and no negligible effects in MRT at the borders of the illuminated zone. Its effect should always be considered.

An important subject of this work has been to analyse the effect induced by a silicon detector in the measurement of a dose profile. We demonstrated that a silicon detector induces a distortion in the experimental data, which can be estimated by EGS4 MC simulations. In conclusion to compare dosimetry measurements with computational predictions a full simulation of the experimental set up has to be performed with an accurated treatment of the detector geometry. In future works some other improvements respect our calculations could be envisaged. It will be desirable to use more realistic phantoms to better simulate the geometry and compositions (cerebral tissue, tumor tissue, skull, etc.) of the infant head. Moreover a method to implement accurately the elastic photon scattering at small angles will certainly need an experimental database of cross sections.

References

1. Laissue J.A., Blattmann H., Di Michiel M., Slatkin D.N., Lyubimova N., Guzman R., Zimmermann W., Birrer S., Bley T., Kircher P., Stettler R., Fatzer R., Jaggy A., Smilowitz H.M., Brauer E., Bravin A., Le Duc G., Nemoz C., Renier M., Thomlinson W., Stepanek J. and Wagner H.P., SPIE Conference Proceeding Vol. 4508, pp. 65-73 (2001).
2. Dilmanian F.A., Button T.M., Le Duc G., Zhong N., Peña L.A., Smith J.A.L., Martinez S.R., Bacarian T., Tammam J., Ren B., Farmer P.M., Kalef-Ezra J., Micca P.L., Nawrocky M.M., Niederer J.A., Recksiek F.P., Fuchs A. and Rosen E.M., Neuro-Oncology **4** (2002a) 26-38.
3. Slatkin D.N., Spanne P., Dilmanian F.A. and Sandborg M., Med. Phys. **9** (1992) No 6.
4. Stepanek J., Blattmann H., Laissue J.A., Lyubimova N., Di Michiel M., and Slatkin D.N., Med. Phys. **27** (2000) No.7,.
5. Orion I., Rosenfeld A.B., Dilmanian F. A., Telang F., Ren B. and Namito Y., Phys. Med. Biol. **45** (2000) 2497-2508.
6. Brauer-Krisch E., Bravin A., Lerch M., Rosenfeld A., Stepanek J., Di Michiel M., Laissue J. A., Med. Phys. **30** (2003) No 4.
7. Nelson W.R., Hirayama H. and Rogers D.W.O., Stanford Linear Accelerator Center Report SLAC-265 (Stanford Colif) (1985).
8. Rosenfeld A., Kaplan G., Kron I., Allen B., Dilmanian F.A., Orion I., Ren B. and Lerch M., IEEE Trans. Nucl. Sci. **46** (1999) 1774.